

Epidemic spreading on preferred degree adaptive networks

Shivakumar Jolad, Wenjia Liu, B. Schmittmann, and R. K. P. Zia

Department of Physics, Virginia Tech, Blacksburg, VA 24060

(Dated: July 21, 2022)

We study the standard SIS model of epidemic spreading on networks where individuals have a fluctuating number of connections around a preferred degree κ . Using very simple rules for forming such preferred degree networks, we find some unusual statistical properties not found in familiar Erdős-Rényi or scale free networks. Preferred degree networks with adaptive κ provide a natural platform to study adaptive contact processes. By letting κ depend on the fraction of infected individuals, we model the behavioral changes in response to how the extent of the epidemic is perceived. Specifically, we explore how various simple feedback mechanisms affect transitions between active and absorbing states. For the static case, we find that the infection threshold follows the heterogeneous mean field result $\lambda_c = \langle k \rangle / \langle k^2 \rangle$ and the phase diagram matches the predictions of the annealed adjacency matrix (AAM) approach. For the adaptive SIS case we find, surprisingly, that even when the average degree shifts, the epidemic threshold does not change. However, the infection level is substantially altered in the active state. A simple mean field analysis is shown to capture the qualitative and some of the quantitative features of the infection phase diagram.

I. INTRODUCTION

Concepts and tools from network science provide a powerful framework for the description of many physical, biological, and social systems, from the world wide web to neural architectures and from Facebook to power grids [1, 2]. Yet, many of the underlying fundamental aspects of networks remain poorly understood. Does function really follow from topology in, e.g., biological networks? How can we use network science to manage critical infrastructures, such as airline networks or power grids, better? Can emerging leaders or ideas be identified from structural features of social networks and from information flow patterns?

Recent years saw an explosive growth of work on time-dependent processes on complex networks [3, 4]. However, in much of this work, the network itself remains static and just provides the structural context (a topology) on which a dynamical process occurs. We refer to this type of study as “dynamics *on* networks.” If the network itself becomes dynamic, by creating or deleting links or nodes, one investigates the “dynamics *of* networks.” The next level of complexity involves *adaptive* networks: here, the dynamics of the variables on the nodes or links is coupled to the dynamics of the network itself, so that a non-trivial feedback loop emerges.

In this work, we study the spreading of an infectious disease on a network of interpersonal connections where the adaptive behaviors of the affected population influence both the disease dynamics and the network topology. If the network of connections were to remain fixed, we would simply be studying yet another example of “dynamics *on* networks.” If new connections are established in the community, or old connections broken, but without any reference to the disease, we would be focusing on another model for the “dynamics *of* networks.” Here, however, we will investigate a situation where, upon hearing news of the outbreak or meeting infected individuals, healthy people modify their behavior, leading to changes

of the network which, in turn, affect the propagation of the disease. The dynamics *on* the network becomes coupled to the dynamics *of* the network. Models of this type are termed *adaptive* or *co-evolving*.

In classic epidemic models such as the susceptible-infected-susceptible (SIS) model and the susceptible-infected-recovered (SIR) model, the spreading of the disease depends on the infection rate λ , the recovery rate μ , and the network of human physical interactions [5, 6]. In the SIS model, susceptible (S) individuals become infected with rate λ upon contact with an infected (I) person and, once infected, re-enter the pool of susceptibles with rate μ . In the SIR model, infected individuals recover (R) from the disease with some rate μ , gain immunity and subsequently do not contribute to the disease dynamics any further. In the following, we focus on SIS models.

The behavior of such classic models has been widely studied on regular lattices and on specific networks such as random or scale-free networks [4, 7, 8]. These studies assume that the disease spreads on a static human network whose members do not change their behavior at the onset of epidemic [9]. However, humans respond with behaviors such as social distancing and quarantine that are perceived to reduce epidemic spread. Such behavioral adaptations invariably change the network topology and feed back into the dynamics of epidemic spreading. Recently, there has been growing interest to include human adaptive behavior in epidemic models. Given the wide range of human adaptations and how they can impact the spread of the disease, modeling all these possibilities seems like a difficult and daunting task. Adaptive epidemic models try to capture these behavioral patterns and their effects in a few effective parameters that significantly impact the dynamics of epidemics. While these models may not reflect all epidemiological or social details in a quantitative fashion, they may be able to provide insight into qualitative and universal features. Funk *et al* [10] classify the current literature based on

the source of information (local or global) and the type of information (belief or prevalence) about the epidemic. Belief-based models emphasize individuals' awareness of a disease, and how they evaluate the associated dangers [11–14]. For example, some authors have modeled risk perception by decreasing the infection rate with the fraction of infected individuals in the local network of the node [15] and by introducing voluntary vaccinations [16, 17]. Prevalence-based models emphasize the objective assessment of the extent of epidemic spread and personal risk. Most of these studies have concentrated on coupling disease dynamics with network adaptations through rewiring of links [18–24] and studying the dynamics of S-I, S-S and I-I links. One might argue, however, that such rewiring models make a somewhat unrealistic assumption, namely, that individuals necessarily create a link with a healthy person after cutting a link with an infected one.

We address some of the limitations of prevalence-based epidemic studies by proposing a new type of network, which is suitable for studying more realistic situations and lets us easily impose adaptive behaviors on the network topology. Our model is more realistic in two aspects: First, we consider networks which more closely resemble a set of social contacts. Unlike scale-free networks, ours has no hubs with unrealistically large degrees (which are responsible for epidemics with vanishing thresholds [25]). Instead, nodes have a *preferred* degree (i.e., individuals have a preference for a certain number of contacts, or “friends”), so that the network topology is similar to that in the simple random case. As will be shown, our model can easily be generalized to endow different nodes with different preferred degrees – a network inspired by the presence of, say, extroverts and introverts [29] in our society. Second, our network is *adaptive*, i.e., it allows us to model a natural human response to the onset of an epidemic, namely, reducing one's number of contacts.

We begin by modeling the simplest case, where all nodes are characterized by a single preferred degree, κ . The network is dynamic, so that nodes can add or delete links, in an attempt to reach or maintain κ . When a disease spreads on this network, the detailed dynamics of adding/removing links changes in response to the epidemic. In the following, we propose a model reflecting *global prevalence-based* information, by letting κ depend only on ϕ , the fraction of I 's in the entire population. Here, we investigate several type of such behavior, from the reckless (where κ remains constant, then drops abruptly when ϕ reaches some threshold) to the nosophobic (who cut ties precipitously as soon as ϕ deviates from zero). We will also briefly touch upon the role of noise, i.e., the effects of adding some random η to ϕ when a node takes adaptive action. Of course, an individual may base his/her response on the level of infection amongst the circle of friends, instead of relying on the media-provided information on the global ϕ . Another aspect of real responses is that the *perceived* infection level may differ

from the *actual* one, ϕ . In future work, we plan to study other adaptive behaviors, including such local- or belief-based models. In this study, our main focus will be the effects of various adaption strategies on the level of infection, ϕ , as the infection rate λ increases.

Our paper is organized as follows: In section II, we set the scene: presenting the formation of preferred degree networks and introducing an SIS dynamics on this network (initially with no adaptive features). We will summarize two theoretical approaches: a simple-minded mean field theory and the more sophisticated annealed adjacency matrix (AAM) method [26]. Let us also mention the heterogeneous mean field theory [27, 28] which has been widely applied to study critical properties near the transition. Since our focus is the bulk of the phase diagram, we will be using only one prediction from this theory, i.e., the critical λ_c . In section III, we turn to adaptive networks, with three prevalence-based responses (coined fear factors). The SIS phase diagram and degree distribution for these adaptive cases are much richer than those in non-adaptive networks. Much of the phase diagram is captured quite well by a simple mean field theory. We conclude, in the last section, with a discussion of our results and their implications for future research.

II. SIS ON PREFERRED DEGREE NETWORKS

A. Network formation

To explore the behavior of epidemics on dynamic networks, let us first discuss how to set up a preferred degree networks. Following the lines introduced in [29], we briefly review how such a network is formed and evolves. Details of the statistical properties of such networks are of interest, but will be deferred to another publication [30]. For simplicity, we consider a system with N nodes (individuals) of identical behavior, evolving stochastically as follows. In each time step, a random node i ($= 1, 2, \dots, N$) is selected and its degree, k_i , is noted. Then, an attempt to add/cut a link is made, with probability $w_+(k_i) / w_-(k_i)$. Clearly, an infinite variety of w_{\pm} 's is possible. In all our simulations, we chose $w_+(k)$ to be a Fermi-Dirac function:

$$w_+(k) = \frac{1}{1 + e^{(k-\kappa)\xi}}, \quad (1)$$

and, to keep the model simple, $w_-(k) = [1 - w_+(k)]$. With this choice of w_- , the network configuration will always change, by the addition or deletion of a link. Here, ξ plays the role of inflexibility or rigidity, so that a node (individual) with $\xi = \infty$ will always cut/add a link when it finds itself with more/fewer links than κ . (In simulations, we choose κ to be slightly larger than an integer, so that no ambiguity should arise.) The partner node for this action is randomly chosen out of the eligible pool. Thus, the recipient node has no control over a link to it, whether created or destroyed. In a Monte Carlo step

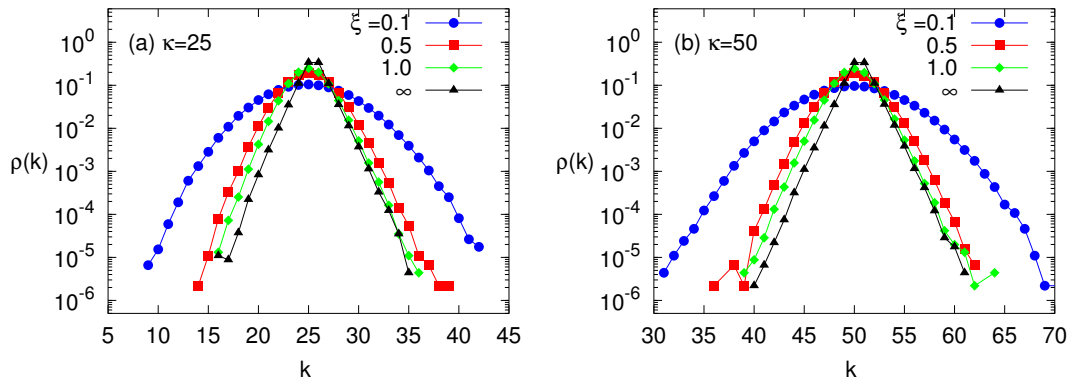


FIG. 1: [Color online] Degree distribution of preferred degree networks with $N = 5000$ for various inflexibility parameters ξ (see Eq. 1). The $\xi \rightarrow \infty$ corresponds to the totally inflexible individuals, and follow Laplace distribution.

(MCS), N such attempts are made, so that there is one chance, on the average, for each node to be chosen to add/cut its links.

With a preferred degree, our network is clearly not scale-free. Also, unlike the case of a Erdős-Rényi network, the degree distribution, $\rho^*(k)$, here is *not Gaussian*. Though it depends on the functions $w_{\pm}(k)$, we discover a universal feature: exponential tails when k is far from κ . In Fig. 1, we show simulation results for ρ^* , in the steady state (with $N = 5,000$ and $\kappa = 25, 50$). Indeed, for a group of rigid individuals ($\xi \rightarrow \infty$), $\rho^*(k)$ is a Laplace distribution ($\propto 3^{-|k-\kappa|}$). With a more flexible group, the maximum around κ is softened to be more Gaussian, up to a width of $\approx 1/\xi$, before crossing over to the exponential tails. This behavior can be heuristically understood [30, 31] in the context of an approximate master equation (expected to be crudely valid near the steady state) for $\rho(k, t)$:

$$\begin{aligned} \Delta\rho(k, t) &\equiv \rho(k, t+1) - \rho(k, t) \\ &\propto \left[w_-(k+1) + \frac{1}{2} \right] \rho(k+1, t) \\ &\quad + \left[w_+(k-1) + \frac{1}{2} \right] \rho(k-1, t) \\ &\quad - [w_+(k) + w_-(k) + 1] \rho(k, t). \end{aligned}$$

The steady state solution of this equation satisfies

$$\frac{\rho^*(k+1)}{\rho^*(k)} = \frac{2w_+(k) + 1}{2w_-(k+1) + 1}$$

and provides remarkably good agreement with simulation data [30, 31].

In addition to a dynamic network, we now endow the nodes with their own degrees of freedom, i.e., a binary state variable: $n_i = 0, 1$ for the node at site i being susceptible or infected. For the convenience of the readers, let us first briefly summarize the properties of SIS dynamics on a similar, but *static*, network and then compare the results with those in our dynamic network.

B. SIS on static and dynamic networks with a preferred degree

For standard evolution dynamics of an SIS model, we randomly choose a node for updating. If it is infected, then it recovers (i.e., n flipped from 1 to 0) with probability μ :

$$I \xrightarrow{\mu} S. \quad (2)$$

If it is susceptible, then the disease is transmitted with probability λ from each of its infected contacts:

$$S + I \xrightarrow{\lambda} I + I. \quad (3)$$

In this simultaneous event, a susceptible node with m infected contacts will contract the disease with probability $1 - (1 - \lambda)^m$ ($\approx m\lambda$ when $m\lambda \ll 1$). Again, a MCS is defined as N attempts at updating a randomly chosen node. Obviously, whether the epidemic dies out or not will depend on network topology and the ratio λ/μ . For simplicity, we fix $\mu = 0.5$ in all our simulations and use λ as a control variable. For our *static* networks, we generated 50 realizations using the scheme specified above (using 10K MCS for each run).

A good measure of the level of the epidemic is $\phi \equiv \sum_i n_i / N$, the fraction of infected nodes. Clearly, a population with $\phi = 0$ will not evolve, i.e., it is in an absorbing state. In general, there is a non-vanishing probability that a finite system will fall into this state in a long run. To facilitate simulations, we artificially prevent the system from becoming static by introducing a trick, through an immortal I . Specifically, we set $\mu = 0$ whenever $\sum_i n_i = 1$, ensuring that the last infected individual never recovers. With this trick, there is no absorbing state. Instead, a disease-free population (for small λ/μ) appears as a non-trivial steady state, with an exponentially distributed ϕ , of width $\mathcal{O}(1/N)$ extending from $\phi = 0$. Of course, for large enough infection rates, the steady state is active, with an average ϕ of $\mathcal{O}(1)$. In all our simulations, we perform long runs with the initial configuration consisting of a single I , and, once the

steady state is reached, measure time averages of ϕ . Except near the transition, the fluctuations over a run are about 1%. The averages from the 50 realizations also do not differ by more than this amount. Not surprisingly, close to the transition, fluctuations are more substantial ($\sim 10\%$). Exploring the critical region quantitatively is a worthwhile pursuit, but beyond the scope of this study. The results of the (quenched) average ϕ vs. λ are shown as solid (blue on line) triangles in Fig. 2 and display a clear signal of the expected transition from inactive to active regimes of the epidemic.

Turning to a dynamic network, we note that, typically, network and disease dynamics proceed at different time scales in nature. It is reasonable to assume that network timescales are slower. In this spirit we choose to update the nodes τ MCS between each update of the network. Mostly, we use $\tau = 10$. Since the network is dynamic, many realizations of our network already appear in a single run. Thus, there is no need to perform 50 runs to arrive at a understandable average for $\phi(\lambda)$. Presented as open squares (black) in Fig. 2, this data show that the average behavior of the epidemic in dynamic and quenched random networks are essentially indistinguishable. It is possible that more discernible differences will appear for systems with smaller N and/or κ . But those issues are also outside the scope of the study here.

C. Simple mean field theory and the annealed adjacency matrix approach

It is possible to understand, to an excellent degree, how the fraction of the infected depends on the rate of infection, $\phi(\lambda)$, by a simple mean field (MF) argument. Typically, such approaches are based on the assumption that the system is homogeneous, and provide good hints of the systems behavior (especially for $N \rightarrow \infty$). Clearly, for fixed μ and small enough λ , the epidemic dies out and the system remains in the $\phi = 0$ branch. Above some critical value, λ_c , it is possible to have $\phi > 0$. On this branch, the recovery rate, $\mu\phi$, just balances the infection rate:

$$\mu\phi = (1 - r)(1 - \phi), \quad (4)$$

where

$$r = (1 - \lambda)^{\kappa\phi} \quad (5)$$

is the probability that an S is *not* infected by any of its infected contacts. Thus, we find the simple MF prediction

$$\lambda_c^{MF} = 1 - e^{-\mu/\kappa}, \quad (6)$$

which reduces, for $\mu \ll \kappa$, to an easily understandable result: $\lambda_c^{MF} \simeq \mu/\kappa$. Now, $\phi(\lambda)$ is given by the solution to Eqn. (4). In other words, it is the inverse of the explicit $\lambda(\phi)$:

$$\lambda^{MF} = 1 - \left\{ \frac{1 - (1 + \mu)\phi}{1 - \phi} \right\}^{1/\kappa\phi}. \quad (7)$$

The result is presented as the solid line (magenta on line) in Fig. 2 and shows that, while slightly higher than the simulation results, it indeed captures the essentials of the epidemics. In the vicinity of criticality, $\phi \ll 1$ and we find $\lambda^{MF} - \lambda_c^{MF} = e^{-\mu/\kappa}(\mu/\kappa)[1 + \mu/2]\phi + \dots$, so that the exponent in $\phi \propto (\lambda - \lambda_c)^\beta$ takes the expected value $\beta = 1$. Note that, for predicting the threshold, this simple theory performs exceedingly well.

Of course, in a dynamic or a quenched random network, this approach may seem too simplistic. In previous studies of SIS models on irregular, static networks, better approximations have been developed. Examples include the *heterogeneous* mean field theory [27, 28] and the annealed adjacency matrix (AAM) approach [26]. The former takes into account a distribution of degrees, such as $\rho^*(k)$ in our case, and provides the critical threshold at $\lambda_c = \mu\langle k \rangle / \langle k^2 \rangle$, i.e., $\lambda_c = \frac{\mu}{\langle k \rangle} / \left\{ 1 + \frac{\Delta k^2}{\langle k \rangle^2} \right\}$. It has been widely applied, with considerable success, to study critical dynamics on various networks. For our study here, we present in Fig. 1 the few cases of $\rho^*(k)$ for the preferred degree networks used, showing that $\langle k \rangle = \kappa$ as expected and $\Delta k^2 / \langle k \rangle^2 \lesssim 1\%$. Since we chose $\mu = 0.5$ for our simulations, the simple MF prediction ($\lambda_c^{MF} \simeq \mu/\kappa$) is quite adequate. Further, as our interest lies in the dominant behavior of the epidemic over the entire phase diagram, rather than details of the transition, there is no compelling need for using this complex method.

As our network is dynamic, we believe that the annealed adjacency matrix method may be most appropriate. Let us briefly summarize this approach [26] here. While the full dynamics involves a fluctuating adjacency matrix A , the matrix element A_{ij} in the AAM is replaced by an average probability that a connection exists between nodes i and j (within the ensemble constraints). For a general network with degree sequence $\{k_1, k_2, \dots, k_N\}$, the AAM element is given by,

$$A_{ij} = A_{ji} = \frac{k_i k_j}{2L} \quad (8)$$

where $L = \sum_i k_i / 2$ is the total number of links. Thus, q_i , the probability that node i is infected evolves according to a discrete Markov equation

$$\Delta q_i(t) \equiv q_i(t+1) - q_i(t) = -\mu q_i(t) + (1 - q_i(t))[1 - r_i(t)]. \quad (9)$$

Here r_i is the probability that this node is *not* infected by any neighbor:

$$r_i(t) = \prod_{j=1}^N [1 - \lambda A_{ij} q_j(t)]. \quad (10)$$

Applying this technique to our problem, we first form a preferred degree network as prescribed above and record its degree sequence. Then we evolve Eq. 9 until it reaches an approximately steady state, $\{q_i^*\}$, and obtain ϕ as the average $\sum_i q_i^* / N$. Then we repeat this procedure 50 times (i.e., with 50 different sequences) and average over

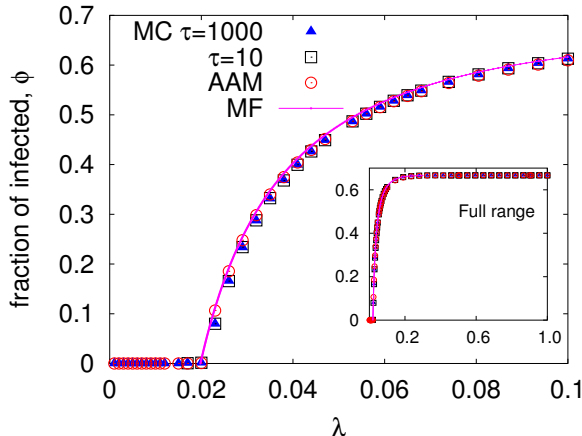


FIG. 2: [Color online] SIS phase diagram near transition point $\lambda_c = 0.02$, comparison with mean field theories. We have set the parameters: $N = 5000$, $\kappa = 25$ and $\mu = 0.5$. τ represents time scale of network updates compared to SIS dynamics. Solid triangles (blue) represent the Monte-Carlo simulation results for quenched network. Results for dynamic network with short network update time scale is shown in black squares. Open circles (red) represent the results of numerically integrating annealed adjacency matrix equations (Eq. 9) and solutions of simple mean field equation (Eq. 7) are plotted as solid lines (magenta).

these 50 ϕ 's. The results are shown as open circles (red on line) in Fig. 2. It is clear that the AAM produces essentially the same $\phi(\lambda)$ as MF theory, and that both are just negligibly higher than either of the two sets of Monte Carlo results (quenched random averages or a dynamic network with $\tau = 10$). Finally, we present the remainder of the $\phi(\lambda)$ curve in the inset of Fig. 2, but only for the AAM and the static network case. As expected, the infected fraction simply saturates at

$$\phi_m \equiv \phi(1) = 1/(1 + \mu). \quad (11)$$

Clearly, the agreement is good over the entire range. Thus, as a first step towards understanding epidemics on more complex, adaptive networks, we will rely on the simpler MF theory. When further detailed properties are sought, we will turn to more sophisticated methods such as the AAM.

Finally, we note that the MF prediction tends to lie slightly above simulation data. Since we expect little correlation in our system, we suspected effects of finite N . However, simulations with systems with N 's as low as 100 in the non-adaptive networks indicate that these deviations appear to saturate at these levels for $N = 500-5000$. Whether such systematic deviations are meaningful remains an interesting question.

III. EPIDEMICS IN AN ADAPTIVE NETWORK

In the networks, whether static or dynamic, presented above, the degree of each node is effectively fixed in time, controlled by an individual's preference for connections. However, when an epidemic is present, individuals are likely to alter their behavior, by cutting ties or reducing the number of non-essential contacts. Such social distancing responses are inherently natural for individuals, as well as the result of an externally imposed public policy (e.g., closure of Singapore primary schools in light of SARS [32]). Further, we believe that cutting down on the number of contacts is a more natural response than rewiring (from an infected to a healthy friend) [18–24], especially if the infection is not easily detectable (e.g., AIDS). Thus, we model adaptive behavior here by letting the preferred degree, κ , change in response to the level of the infection. In this work, we will focus on the effects of the various feedback mechanisms on the epidemic (in steady states). In particular, we investigate $\phi(\lambda)$ as well as the degree distributions, $\rho^*(k)$.

A. Simple models of adaptive behavior and the effects on infection levels

When an individual becomes aware of an epidemic, the response can be the product of rational/prudent behavior or irrational perceptions of the dangers (fear factors). In addition, a typical population is diverse and heterogeneous, as different individuals respond in different ways. For simplicity and as a first step in a study of adaption, we focus on a homogeneous population (one κ for all individuals) whose only information of the epidemic is the global infection level (i.e., ϕ). Thus, this model is more appropriate for a disease like AIDS than for, say, the flu. Let us introduce different kinds of response via a function $f(\phi)$, for which we coin the term fear factor, with the following properties:

$$\begin{aligned} \kappa(\phi) &= \kappa_0 f(\phi) \\ f(0) &= 1, \quad f(1) = \kappa_{min}/\kappa_0. \end{aligned} \quad (12)$$

Here, κ_0 is clearly the preferred degree for a healthy population, while f is most naturally a monotonically decreasing function of the fraction of infected, ϕ , effectively reducing the preferred degree. Of the infinitely many behavioral patterns that can be modeled, we consider only three kinds here (Fig. 4):

- **Reckless** individuals are oblivious if a low level of epidemic is present in the population. They do not cut links until the epidemic reaches a certain threshold: ϕ_θ . (Of course, we assume ϕ_θ to be some fraction of ϕ_m .) At this point, they abruptly change their preferred degree to κ_{min} . Keeping in mind that a typical person would maintain a

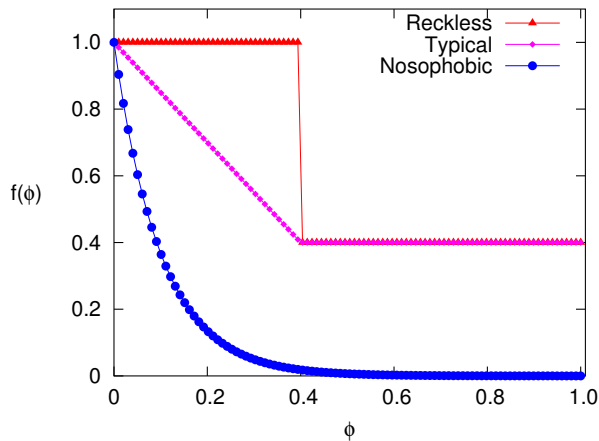


FIG. 3: [Color online] Adaptive “fear factor” $f(\phi)$ (see Eq. 12) associated with different behavioral patterns listed in section III.A .

minimal set of contacts (family, caretakers, etc.) even in the face of a raging epidemic, we simply choose κ_{min} to be independent of ϕ for all levels higher than ϕ_θ . Explicitly, $f_{reckless}(\phi) = \Theta(\phi_\theta - \phi) + (\kappa_{min}/\kappa_0) \Theta(\phi - \phi_\theta)$, where Θ is the Heaviside step function. For simulations, we choose $\phi_\theta = 0.4, \kappa_0 = 25, \kappa_{min} = 10$.

- **Typical** individuals are likely to cut their contacts in a more measured fashion. For them, we choose a linearly decreasing $f(\phi)$. If this decrease is rapid enough, then these individuals’ comfort level would reach the lower limit (κ_{min}) before the infection rate reaches unity (and ϕ arrives at ϕ_m). Again for simplicity, we let their κ remain at κ_{min} for all higher levels of infection. Explicitly, $f_{typical}(\phi) = (1 - \alpha\phi) \Theta(\phi_\theta - \phi) + (\kappa_{min}/\kappa_0) \Theta(\phi - \phi_\theta)$, where the slope and the threshold are related by $\alpha\phi_\theta = 1 - \kappa_{min}/\kappa_0$. For this set of simulations, we chose the same parameters as above: $\phi_\theta = 0.4, \kappa_0 = 25, \kappa_{min} = 10$.
- **Nosophobia** is an irrational fear of contracting diseases. To model such a population, we let f drop exponentially, as soon as the slightest infection is detected. These individuals would eventually avoid all personal contact – decontaminating all food delivered to them, etc. Explicitly, we have $f_{nosophobic}(\phi) = \exp(-\phi/\phi_s)$. With ϕ_s setting the severity of this phobia, we use $\phi_s = 0.1$ in our simulations.

Setting aside the interesting question of how ϕ changes with time as a result of a changing network topology (in response to the feedback from $\kappa(\phi)$), we focus on the steady states after the system settles down. In Fig. 4, we show the simulation results for $\phi(\lambda)$ in these three cases (with mostly $\xi = 1$, flexible individuals, for simplicity), as well as the case above: a non-adaptive network. For the last group, we coin the term fearless and

write $f_{fearless} = 1$, depicting their undaunted nature, regardless of the level of the infection. We first observe that the epidemic thresholds are essentially unchanged by any of the adaptive strategies. This fact is understandable, since the threshold is defined by ϕ rising from zero and our transition is continuous. Thus, fear in the population has yet to take hold, and κ remains close to κ_0 . Beyond the threshold, the effects of the different fear factors are self-evident. The reckless follow the fearless until ϕ reaches ϕ_θ (chosen to be 0.4 here), and then abruptly adjust their response so that the infection remains more or less at this level. In the inset, we see that ϕ resumes its upward trend after $\lambda \simeq 0.1$, and reaches close to the maximal level $\phi_m = 2/3$ by $\lambda \simeq 0.5$. By contrast, the infection level in the typical case increases at a slower pace immediately after λ_c . Around $\lambda \simeq 0.1$, $\phi_{typical}(\lambda)$ coincides with the reckless, since both networks are controlled by the same $\kappa_{min} = 10$. Finally, as expected, infections in a nosophobic population are strongly suppressed. Indeed, the critical properties near the transition may be altered. Since $\kappa(\phi)$ is effectively zero for $\phi \gtrsim \phi_s \ln \kappa_0$ (i.e., $0.1 \ln 25 \simeq 0.35$ here), it is not surprising that the infection levels are far lower than the other two types.

More quantitatively, simple MF theory should provide an acceptable explanation for these results. From the analysis above, a $\kappa(\phi)$ can be readily incorporated, so that λ_c^{MF} remains unchanged: $1 - e^{-\mu/\kappa_0}$. Above this value, the only modification is the λ - ϕ relationship, and Eqn. (7) now reads

$$\lambda^{MF} = 1 - \left\{ \frac{1 - (1 + \mu)\phi}{1 - \phi} \right\}^{1/(\kappa_0 \phi f(\phi))}. \quad (13)$$

Although the fear factor appears explicitly here, this expression is quite cumbersome. A simple way to regard the effects of adaptation is the following: To produce the same level of infection (ϕ), the infection rate (λ) must be enhanced over the non-adaptive, fearless population. Quantitatively, $-\ln(1 - \lambda)$ ($\cong \lambda$, for small λ such as in our examples) must increase by a factor of $1/f(\phi)$. In this way, it is easy to see that the MF prediction of the critical exponent β will remain unchanged, unless f is appropriately non-analytic at $\phi = 0$ (i.e., $\beta = \beta'$ if $1 - f \propto \phi^{\beta'}$ with $\beta' < 1$). At the other extreme, the saturation levels are given by setting the left side of Eqn. (13) to unity. Unless the fear factor is so intense that f vanishes at a value of ϕ less than $1/(1 + \mu)$, then, strictly speaking, these do not depend on the details of the adaptive strategy $f(\phi)$. However, for the severely fearful such as the nosophobic, the infection essentially levels off at a ϕ considerably lower than ϕ_m . As an illustration, when λ comes within 10^{-10} of unity in our specific nosophobic sample, ϕ is just 0.57, a value considerably lower than $\phi_m = 2/3 \cong 0.67$.

Comparing with simulation data, we see that the MF predictions (Fig. 4) tend to lie a little above simulation data. There are two notable exceptions. One is the nosophobic case, at large λ (e.g., $\lambda = 0.44$). Here, as we see from simulations, $\phi \cong 0.24$, which implies that the fear

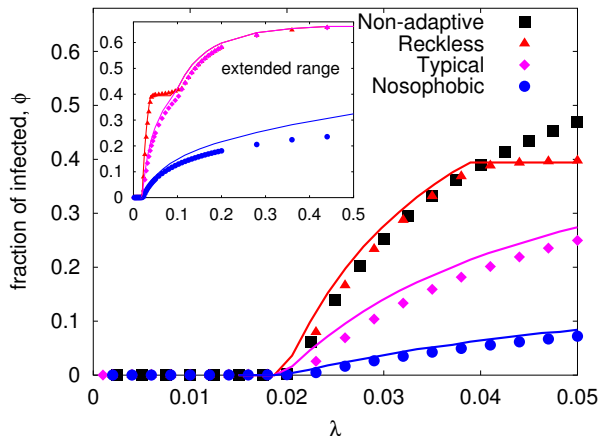


FIG. 4: [Color online] Non-adaptive (fearless) and adaptive preferred degree SIS phase diagram. We have chosen $N = 5000$, $\kappa_0 = 25$ and $\kappa_{min} = 10$ for all three adaptive models (See Fig. 3). The solid lines represent the mean field solution to these models based on Eq. 13.

factor reduces the preferred degree to 2. In MF theory, this means r , the rate of *not* being infected, is computed with $(1 - \lambda)$ raised to $\kappa(\phi)\phi \sim 2 \times 0.24 \sim 0.5$. But the latter represents the number of infected contacts, which must be integers in a run. If we arbitrarily round off 0.5 to 0, we obviously underestimate the number of infected contacts. As a compromise, a very rough estimate is to average $\kappa(\phi)\phi$ and the next lowest integer (0 in this example). Remarkably, such a rough procedure produces a (self consistent) estimate for ϕ much closer to the observed value. Clearly, a quantitative understanding of the results in this regime will require more care with the discreteness of contact numbers, as well as a more reliable method than simple MF theory.

The other exception is a region associated with the abrupt drop in $\kappa(\phi)$ for the reckless population, where MF results are lower than simulations. We believe this effect may be the result of large fluctuations in the degree distribution. Individuals caught in this regime may cut ties drastically (at the news of ϕ rising above ϕ_θ), causing the infection to decline. But this good news would lead to the population reversing course just as abruptly, so that large fluctuations should continue. To test this conjecture, we present, in the next subsection, degree distributions as an indication of how serious these fluctuations can be.

B. Degree distributions in adaptive networks

In the absence of infection, the degree distribution should be similar to those in Fig.1, around the preferred κ_0 . Far from the transition, the epidemic has settled in and, for both the typical and the reckless, the distribution should also be similar, but settling around κ_{min} instead. Not surprisingly, the picture is more complex for

the nosophobic, especially for large λ , since the preferred degree is strongly dependent on the level of the infection. Here, let us focus on the effects of the abrupt behavior of the reckless, the case that also displays the most interesting behavior (large fluctuations, Fig.5a,b). For the other two types, we note the predictably mild changes in the degree distribution, as λ increases (Fig.5c,d). With the overall shape of $\rho^*(k)$ remaining essentially the same, the only serious effect due to adaptation is the slowly shifting center with ϕ and λ .

For the reckless population, the conjectured behavior – dramatic swings when the infection level is near ϕ_θ – is well captured in the broadening of $\rho^*(k)$. From the data shown in Fig.5a, we see that the distributions are, as expected, centered close to κ_0 for $\lambda \lesssim 0.04$ ($\lambda \sim 0.04$ corresponding to the threshold $\phi_\theta \sim 0.4$). Thereafter, many individuals in the population begin to cut contacts. By $\lambda = 0.05$, $\rho^*(k)$ is quite distorted compared to the simple Laplace distribution. Specifically, we see that a sizable fraction of the population has cut their preferences down towards $\kappa_{min} = 10$. To display a complete range of infection rates, we chose to simulate with rigid individuals ($\xi = \infty$) for simplicity (Fig.5b). Here, we see the complete crossover as λ increases, from a distribution centered around κ_0 to one around κ_{min} . Note that the $\lambda = 0.070$ distribution appears as distorted as the $\lambda = 0.050$ case, but peaked closer to κ_{min} instead of κ_0 . Indeed, if we plot a reflected and appropriately shifted version of the $\lambda = 0.065$ distribution (i.e., $\rho^*(\tilde{k} - k)$ for an appropriate \tilde{k}), the result is essentially identical to the raw $\rho^*(k)$ for $\lambda = 0.050$. A similar collapse is observed for the cases with $\lambda = 0.055$ and $\lambda = 0.060$, $\rho^*(k)$. Thus, we may associate $\lambda_{f-t} \cong 0.057$ with a transition, from a population dominated by κ_0 (i.e., fearless behavior) to one controlled by κ_{min} (i.e., typical). Since $\rho^*(k)$ displays always a single peak, which shifted rapidly between κ_{min} and κ_0 , we would label this as a continuous transition. In equilibrium statistical mechanics, we would characterize a transition as discontinuous only when the distribution (of an order parameter) is bi-modal over a finite interval of the control parameter. Such distributions are typically associated with hysteresis, another hallmark of first order transitions. Here, bi-modal $\rho^*(k)$'s are never observed, while the large fluctuations around λ_{f-t} are reminiscent of those in second order, continuous, transitions. Further extensive simulations are needed to shed better light on these questions.

IV. SUMMARY AND OUTLOOK

Network science has become an integral tool to understand many complex phenomena in the physical and socio-biological sciences. Although the study of dynamical process on networks has been very active for several decades, most investigations focused on either a dynamic set of nodes on a static network (e.g., spins on a lattice

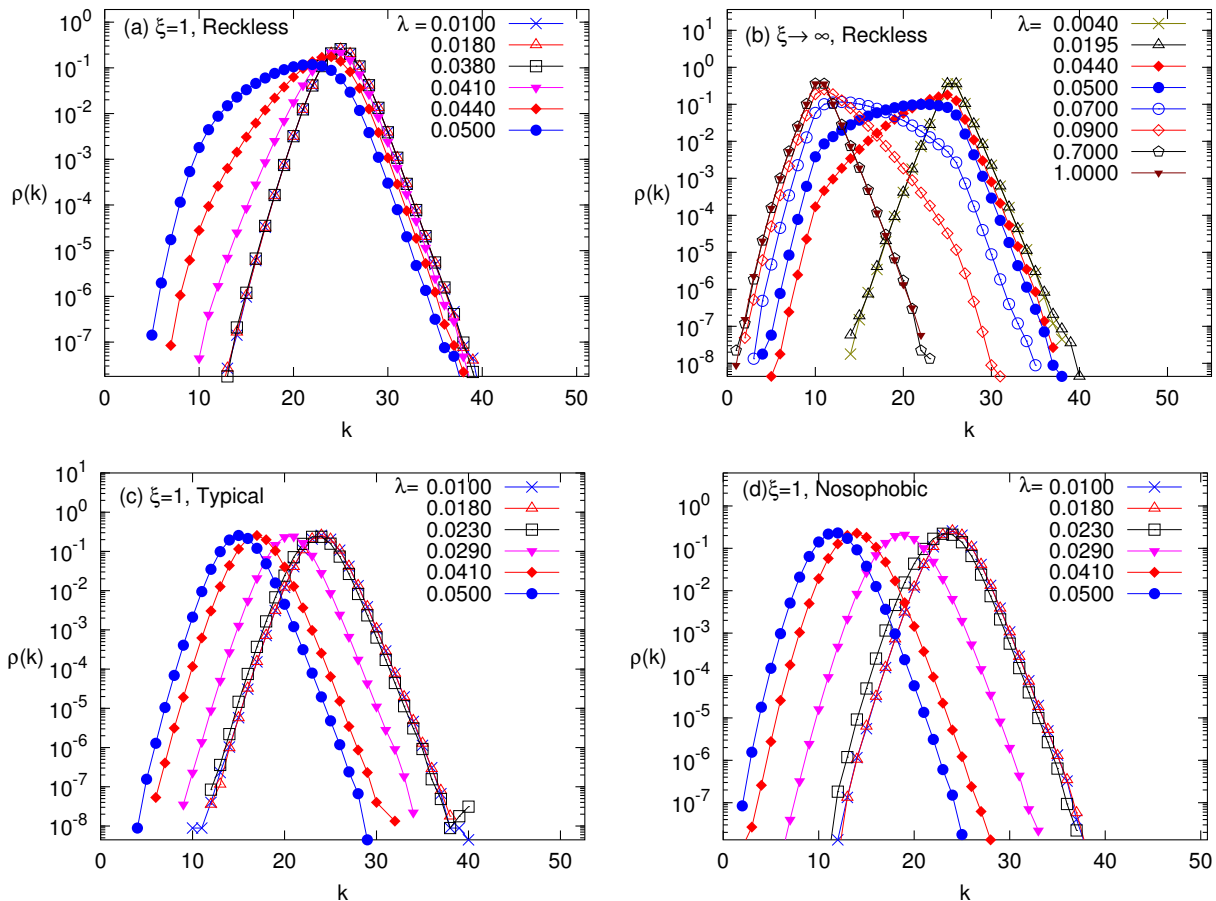


FIG. 5: [Color online] Degree distribution of (a) Reckless with $\xi = 1$ (see Eq. 1) (b) Reckless and inflexible individuals ($\xi = \infty$), (c) Typical and (d) Nosophobic individuals (see Sec 3.A for details) with $\xi = 1$. We have chosen $N = 5000$, $\kappa_0 = 25$, $\kappa_{min} = 10$ for all these cases. The infection rates λ are chosen to illustrate transition behavior in degree distribution.

or epidemics in a population with fixed connections) or a dynamic network with static nodes (e.g., growing small world networks). Here, we study systems in which both nodes and links are dynamic, co-evolving as in many realistic systems. For simplicity, we consider the classic SIS model of epidemic spreading, on a network that adapts to the level of the infection. Introducing a new class of networks in which individuals (nodes) favor a certain number of contacts (κ , the preferred degree), we model various types of adaptive behavior by letting κ depend on the level of the epidemic, through ϕ , the infected fraction of the population. For such networks, we typically find degree distributions that are neither Gaussian nor scale-free. Instead, the universal feature appears to be exponential tails when the degree is far from κ .

Using Monte Carlo methods, we simulated populations in which healthy individuals may become ill by being in contact with a fluctuating set of infected nodes, while diseased persons recover spontaneously with some rate. We considered four types of behavior. The fearless do not adapt, maintaining the same κ regardless of ϕ . This system also provides a baseline with which to compare different adaptive strategies. The reckless behave exactly

as the fearless until ϕ reaches a threshold, then abruptly lower their preference to a fixed minimal level. Modeling a typical person, we let κ decrease gently (linearly) with ϕ until it reaches the minimal κ . Finally, we consider the nosophobic who cut ties as soon as any infections appear, with κ decaying exponentially. Many of the qualitative aspects in the systems we considered are understandable. Quantitatively, good agreement with data can typically be found with a simple mean field theory. Nevertheless, there are several interesting issues which deserve further investigation. In addition, there are many natural generalizations. In the remaining paragraph, let us provide a brief outlook on potentially fruitful avenues of future research.

Within the scope of our study, many extensions can be pursued. Two outstanding questions were noted above: What is the nature of the large fluctuations discovered in the fearless-typical transition? Is it similar to a second order phase transition? and if so, what is its universality class? The other issue concerns the nosophobic when λ is substantial. How can we understand the considerable deviations from MF theory? The role of noisy perceptions is also interesting. In a typical society, the population is

inhomogeneous, so that an individual's perception of the infection level may not be the same as the overall ϕ . Letting the adaptive behavior depend on this perceived level, we consider variations in strategies by simply adding a white noise to ϕ . Our preliminary studies, not reported above, indicate that the effect of this type of noise on the epidemic appears to be minimal. A detailed study is under way and may produce more interesting phenomena. Apart from steady state properties – the main focus of the work here – there must be interesting transient behavior. If an infection suddenly becomes virulent and λ increases, what is the subsequent time dependence, as different populations adapt different strategies in response? Are there oscillations, as the individuals over-react to a large ϕ and, cutting contacts drastically, face a rapidly decaying epidemic? If such phenomena are found, do the time scales depend sensitively on τ ?

Beyond our simple model, the most immediate generalization is to include spatial structures, both homogeneous and heterogeneous. In a real society, behavior is

not uniform across all individuals. For example, extroverts and introverts have very different preferred degrees. How does an epidemic develop across these different communities? There is a general belief that extroverts are more prone to contagious diseases. Perhaps quantitative versions of such statements can be made, within the context of an appropriate set of models. Naturally, the long term interest in such studies is to develop a good understanding so that reasonable public policies can be formulated in response to a real epidemic.

V. ACKNOWLEDGEMENTS

We thank Stephen Eubank, Thierry Platini and Madhav Marate for illuminating discussions. This research is supported in part by grants DMR-0705152 and DMR-1005417 from the US National Science Foundation.

-
- [1] R. Albert and A-L. Barabási, *Rev. Mod. Phys.* **74**, 47 , (2002).
- [2] E. Estrada, M. Fox, D.J. Higham, and G.-L. Oppo (Eds.), *Network Science: Complexity in Nature and Technology* (Springer, New York, 2010).
- [3] S. N. Dorogovtsev, A. V. Goltsev, and J. F. F. Mendes, *Rev. Mod. Phys.* **80**, 1275 (2008).
- [4] A. Barrat, M. Barthelemy, and A. Vespignani, *Dynamical processes in complex networks*, Cambridge University Press, (2008).
- [5] R.M. Anderson and R.M. May, *Infectious Diseases of Humans* (Oxford University Press, New York, 1991).
- [6] D. J. Daley, and J. Gani, *Epidemic Modelling: An Introduction* (Cambridge University Press, 2000) .
- [7] C. Moore and M. E. J. Newman, *Phys. Rev. E* **61**, 5678 (2000).
- [8] R. Pastor-Satorras and A. Vespignani, *Phys. Rev. E* **63**, 066117 (2001).
- [9] J. M. Epstein, *Nature* **460**, 687 (2009).
- [10] S. Funk, M. Salathé, and V. A. A. Jansen, *J. R. Soc. Interface*, **7** (50) 1247 (2010).
- [11] S. Funk, E. Gilad, C. Watkins, and V. A. A. Jansen, *PNAS*, **106** (16) 6872 (2009).
- [12] J. M. Epstein, J. Parker, D. Cummings, and R. A. Hammond, *PLoS ONE*, **3**(12): e3955 (2008).
- [13] M. M. Tanaka, J. Kumm, and M. W. Feldman, *Theor. Popul. Bio* **62**, 111 (2002).
- [14] I. Z. Kiss, J. Cassell, M. Recker, and P. L. Simond, *Mat. Bio. S*, **225** (1), 1 (2010).
- [15] F. Bagnoli, P. Lió, and L. Sguanci, *Phys. Rev. E* **76**, 061904 (2007).
- [16] C. T. Bauch, A. P. Galvani, and D. J. D. Earn, *PNAS*, **100** (18), 10564 (2003).
- [17] A. Perisic and C. T. Bauch, *PLoS Comput Biol* 5(2): e1000280 (2009).
- [18] T. Gross, C. J. D. D’Lima, and B. Blasius, *Phys. Rev. Lett.* **96**, 208701 (2006).
- [19] B. Wang, L. Cao, H. Suzuki, and K. Aihara, *J. Phys. A: Math. Theor.* **44** 035101, (2011).
- [20] D. H. Zanette and S. Risau-Gusmán, *J Biol Phys*, **34**, 135 (2008).
- [21] V. Marceau, P. Noël, L. Hébert-Dufresne, A. Allard, and L. J. Dubé, *Phys. Rev. E* **82**, 036116 (2010).
- [22] T. Gross and I. G. Kevrekidis, *Europhys. Lett.*, **82** 38004, (2008).
- [23] Y. Schwarzkopf, A. Rákos, and D. Mukame, *Phys. Rev. E* **82**, 036112 (2010).
- [24] L. B. Shaw and I. B. Schwartz , *Phys. Rev. E* **77**, 066101 (2008).
- [25] C. Castellano and R. Pastor-Satorras, *Phys. Rev. E* **105** 218701 (2010).
- [26] B. Guerra, and J. Gómez-Gardeñes, *Phys. Rev. E* **82**, 035101(R) (2010).
- [27] R. Pastor-Satorras and A. Vespignani, *Phys. Rev. Lett.* **86**, 3200 (2001).
- [28] Y. Moreno, R. Pastor-Satorras, and A. Vespignani, *Eur. Phys. J. B* **26**, 521 (2002).
- [29] T. Platini and R. K. P. Zia, *J. Stat. Mech.: Theor. Exp.* P10018 (2010).
- [30] Wenjia Liu, Shivakumar Jolad, B. Schmittmann, and R.K.P. Zia, to be published.
- [31] R.K.P. Zia, Wenjia Liu, Shivakumar Jolad, and B. Schmittmann, *Physics Procedia* **15**, 102 (2011).
- [32] Singapore Media release on closing of schools, <http://www.moe.gov.sg/media/press/2003/pr20030326.htm> (2003).